

1 **Impact of Arctic shelf summer stratification on Holocene climate variability**

2

3 Benoit Thibodeau^{1,2,*}, Henning A Bauch³ and Jochen Knies^{4,5}

4

5 ¹Department of Earth Sciences, University of Hong Kong, Pokfulam Road, Hong Kong SAR

6 ²Swire Institute of Marine Science, University of Hong Kong, Cap D'Aguiar, Hong Kong SAR

7 ³Alfred Wegener Institute, Helmholtz Centre for Polar and Marine Research c/o GEOMAR

8 Helmholtz Centre for Ocean Research, Wischhofstrasse 1-3, 24148, Kiel, Germany

9 ⁴Geological Survey of Norway, Trondheim, Norway

10 ⁵CAGE–Centre for Arctic Gas Hydrate, Environment and Climate, Department of Geosciences,

11 UiT The Arctic University of Norway, NO-9037 Tromsø, Norway

12

13

14

15

16 *Correspondence to: Benoit Thibodeau, Department of Earth Sciences, University of Hong Kong,

17 Pokfulam Road, Hong Kong SAR +852 3917 7834 bthib@hku.hk

18

19 Highlights

20

21 • We reconstructed variation in nutrient utilization over the Laptev Sea throughout the
22 Holocene

23 • The Holocene Siberian transgression modulated the water column structure and created
24 unstable conditions in the Laptev Sea until 4 ka

25 • Oceanographic conditions favorable to the onset of the Laptev Sea 'sea-ice factory' were
26 reached around 2 ka

27

28 **Abstract**

29 Understanding the dynamic of freshwater and sea-ice export from the Arctic is crucial to
30 better comprehend the potential near-future climate change consequences. Here, we report
31 nitrogen isotope data of a core from the Laptev Sea to shed light on the impact of the Holocene
32 Siberian transgression on the summer stratification of the Laptev Sea. Our data suggest that the
33 oceanographic setting was less favourable to sea-ice formation in the Laptev Sea during the early
34 to mid-Holocene. It is only after the sea level reached a standstill at around 4 ka that the water
35 column structure in the Laptev Sea became more stable. Modern-day conditions, often described
36 as “sea-ice factory”, were reached about 2 ka ago, after the development of a strong summer
37 stratification. These results are consistent with sea-ice reconstruction along the Transpolar Drift,
38 highlighting the potential contribution of the Laptev Sea to the export of freshwater from the Arctic
39 Ocean.

40

41 **1. Introduction**

42 The Arctic climate is changing at a rapid pace; in fact, this region warms faster than any other
43 on the globe because of polar amplification (Manabe and Stouffer, 1980; Serreze and Barry, 2011).
44 One major impact of the observed warming is the dramatic increase in the sea-ice melt season and
45 the consequent reduction of sea-ice cover (Comiso et al., 2008; Perovich and Richter-Menge,
46 2009). These changes in the sea-ice dynamic directly influence the export of sea-ice via Fram Strait,
47 which accounts for about 25% of the total freshwater export from the Arctic (Serreze et al., 2006).
48 Thus, the Arctic sea-ice export through Fram Strait plays an important role in the global climatic
49 system as it influences the freshwater balance of the northern North Atlantic (Curry, 2005;
50 Sciences et al., 2006), which in turn affects the strength of the Atlantic meridional overturning
51 circulation (Belkin et al., 1998; Dickson et al., 1988; Ionita et al., 2016).

52 From all Siberian shelf seas, the Laptev Sea is thought to contribute the largest fraction of
53 sea-ice export towards Fram Strait (Krumpen et al., 2016; Reimnitz et al., 1994; Zakharov, 1966)
54 (Fig. 1). It was suggested that 20% of the sea-ice transported via the Transpolar Drift (TD) through
55 Fram Strait is produced in the Laptev Sea (Rigor and Colony, 1997) and recent estimates suggested
56 that the Laptev Sea was exporting an area of sea-ice equivalent to 41% of the sea-ice exported via
57 Fram Strait (Krumpen et al., 2013). Thus, it is critical to understand the longer-term dynamics of
58 sea-ice production within the Laptev Sea in order to better apprehend the potential near-future
59 change in sea-ice export via Fram Strait. The presence of a relatively fresh surface layer promotes
60 the formation of ice in the Laptev Sea, which, in turn, releases brines and contributes to the
61 formation of the shelf halocline layer, a critical “buffer” between the surface and the saltier bottom
62 layer (Dmitrenko et al., 2009; Krumpen et al., 2013). The resulting stratification is strong enough
63 to persist through the whole year as the long term probability for winter convection to reach the

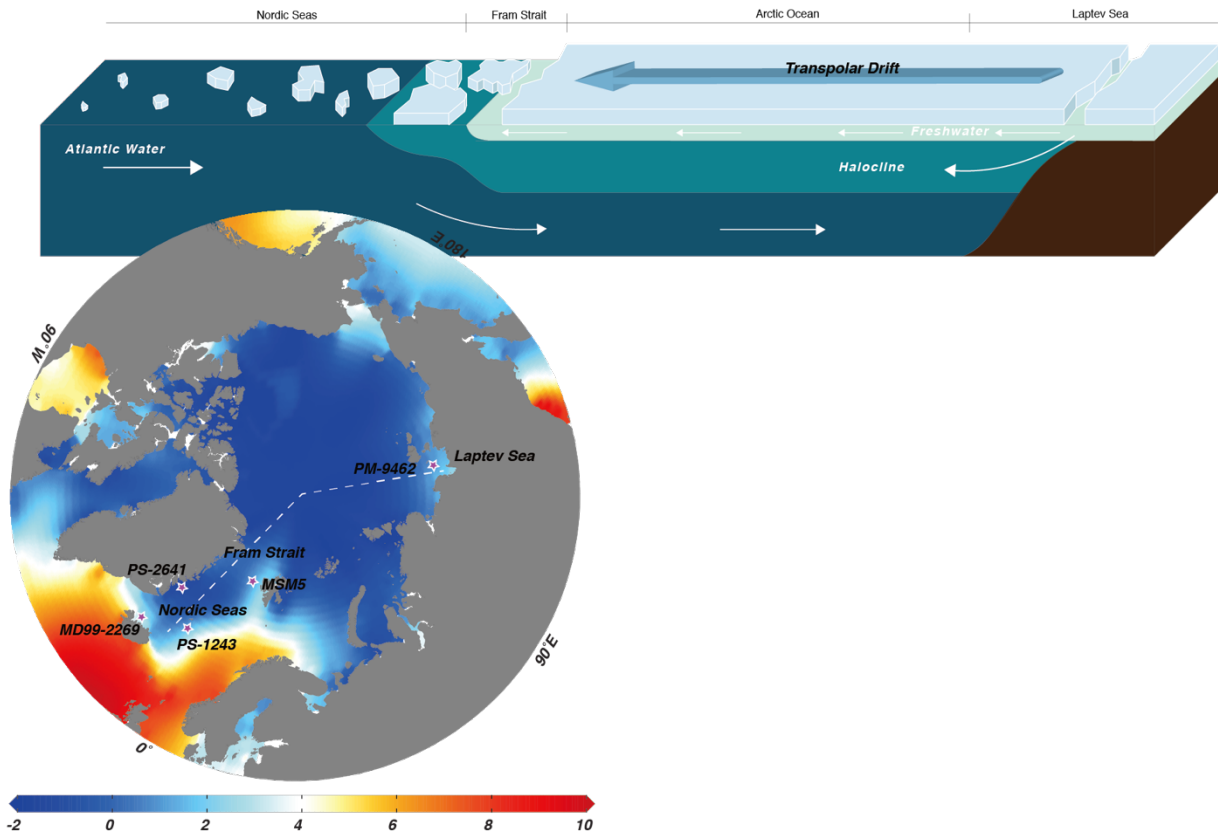
64 seafloor is only about 20 % (Dmitrenko et al., 2012; Krumpen et al., 2011). The strength of
65 stratification is controlled by the summer atmospheric circulation that influences the freshwater
66 budget of the Laptev Sea (Dmitrenko et al., 2005, 2008; Thibodeau et al., 2014) and preconditions
67 the next winter sea-ice production (Bauch et al., 2012; Dmitrenko et al., 2010; Thibodeau & Bauch,
68 2016). Despite the widely recognized climatic importance of the Laptev Sea stratification, we
69 possess no information on its longer-term evolution through the Holocene, i.e., during the past 11
70 ka when post-glacial sea level rise caused dramatic environmental changes on the circum-arctic
71 shelves (Bauch et al., 2001b), and on the role it might have played on the gradual establishment of
72 modern Arctic climate.

73 Recent work based on geochemical proxies reconstructed the Holocene variability in the
74 production of sea-ice algae over the Laptev Sea (Hörner et al., 2016). They observed a general
75 increasing trend superimposed by short-time variability that was interpreted as representing Bond
76 cycles (1500 ± 500 ka), which are generally considered to be linked to changes in solar activity
77 (Bond et al., 1997). However, the 1500-year cycle in Arctic Oscillation and Arctic sea-ice drift
78 was previously found distinct from the solar irradiance cycle and it was hypothesized that internal
79 variability or indirect response to low-latitude solar forcing was driving the cycle (Darby et al.,
80 2012). This is actually in line with the original analysis of Bond et al (2001) who found the last
81 three ice-drift cycles to be discordant with both the Arctic Oscillation and North Atlantic
82 Oscillation dipole anomaly. This highlight the need to investigate other mechanisms that could
83 influence the sea-ice production in the Arctic Ocean over the Holocene, like water column
84 stratification in marginal seas.

85 Here, we use nitrogen isotope in a well-dated sediment core from the Laptev Sea shelf to
86 reconstruct nutrient utilization and summer stratification. Comparison with proxy of sea-ice algae

87 production is carried-out to investigate the link between the stratification and the variation in sea-
88 ice. We will then implicate our record to sea-ice export, temperature and water stratification
89 proxies along the TD to better understand the potential impact of the Laptev Sea stratification on
90 the larger-scale Arctic climate processes.

91



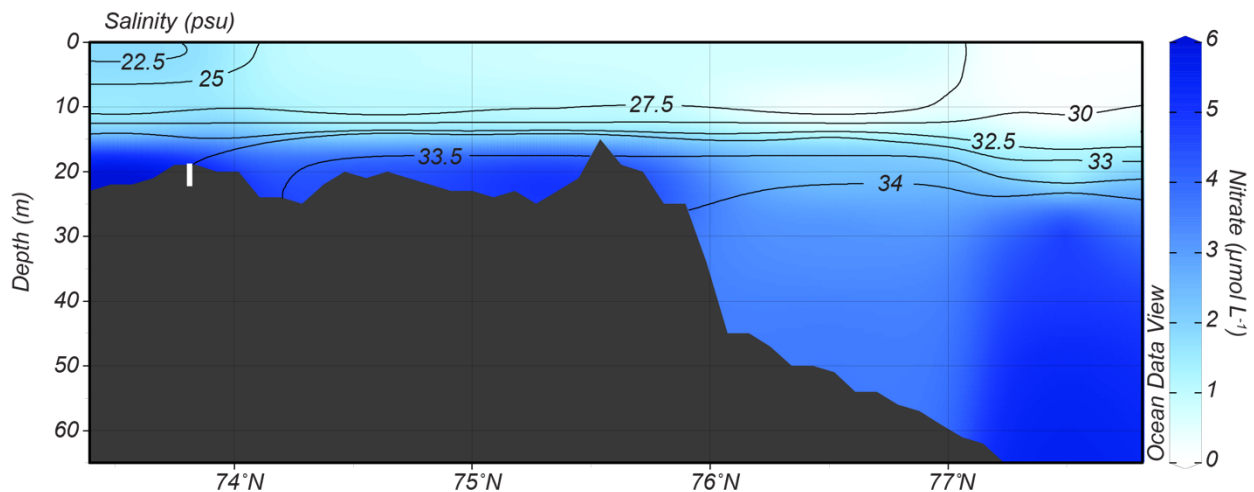
93

94 Fig 1. The Transpolar Drift system from the Laptev Sea to the Nordic Seas. The upper panel is a depth
 95 profile of the different water masses along the white dashed transect on the bottom panel. The color scale
 96 on lower panel shows the 1955-2012-averaged sea-surface January temperature ($^{\circ}\text{C}$) (data from Levitus et
 97 al., 2013). Location of the cores discussed in the paper are indicated by stars on the lower panel.

98

99 **2. Regional Setting**

100 The Laptev Sea is characterized by an estuarine-like circulation, with freshwater runoff from
101 the Lena River at surface and an inflow of salty modified-Atlantic water at depth. This physical
102 feature exerts a strong control on the biogeochemistry of nutrients, notably nitrate (e.g., Kattner et
103 al., 1999). The strong stratification between surface freshwater and marine-derived bottom water
104 prevent any replenishment of nutrients during summer. Thus, nitrate from winter mixing and from
105 the Lena River is rapidly consumed in the surface water during Arctic summer, leading to very
106 low, but not totally depleted, nitrate concentration at the end of the summer ($\sim 0.5 \mu\text{mol L}^{-1}$), while
107 bottom water are between 2 and 6 $\mu\text{mol L}^{-1}$ (Thibodeau et al., 2017a). During winter, mixing
108 occurs and replenishes the surface water with nutrients. The most recent data suggest that the
109 surface water overlying the core today is characterized by nitrate concentration between 1.5 and 2
110 $\mu\text{mol L}^{-1}$ at the end of the Arctic summer (Fig. 2).



111
112 Fig 2. Depth profile of nitrate concentration (color raster) and salinity (black contours) measured in 2014
113 (Thibodeau et al., 2017a) at $\sim 131^\circ\text{N}$, close to the core studied here (represented in white).

114

115 **3. Material and Methods**

116

117 3.1 *Sediment core and chronology*

118 The 467 cm-long vibrocore PM9462 was raised from 27 m water depth in the east part of the
119 Laptev Sea (73°30.2'N, 136°00.3'E). The sediment core was mainly composed of uniform, nearly
120 black, clayey silt (originally described in Bauch et al., 2001b). The chronology of the core was
121 established based on twelve *Portlandia arctica* ¹⁴C measurements (Bauch et al., 2001a). Reservoir
122 age (370 ± 49 ¹⁴C yr B.P.) was determined from the shell of living bivalves from the bottom of
123 the Laptev Sea. Linear interpolation was used to estimate the age between each ¹⁴C value. The
124 oldest measured age is about 8900 cal yr B.P. (Bauch et al., 2001a). Depending on the sample
125 interval, the resolution of each sample ranges from 104 to 391 cal yr.

126

127 3.2 *Geochemical and micropaleontological proxies*

128 Multiples proxies were already available for this sediment core; total organic carbon, δ¹³C or
129 organic carbon, the aquatic palynomorphs (chlorophyceae and dinoflagellates), grain size and
130 garnet content (Fig. 3). Original data and detailed methods can be found in Bauch et al., (2001b).

131

132 3.3 *Organic nitrogen isotope*

133 In this study we use, for the first time, the nitrogen content and nitrogen stable isotope (δ¹⁵N)
134 to investigate the dynamic of nitrogen over this shelf during the Holocene. Nitrogen stable isotope
135 can be used to reconstruct past changes in the nitrogen cycle (e.g., Altabet & Francois, 1994;
136 Galbraith et al., 2008; Robinson et al., 2004; Tesdal et al., 2013). In ecosystems where nitrogen is
137 not fully assimilated, the δ¹⁵N is directly linked to the isotopic signature of the supply of nitrate
138 and the fractionation caused by its assimilation and thus, can be used to highlight potential change
139 in the relative proportion of nitrate that is consumed (N-utilization) (Riethdorf et al., 2016; Straub

140 et al., 2013; Thibodeau et al., 2017b). However, in the Arctic Ocean, an important caveat to the
141 use of bulk sediment $\delta^{15}\text{N}$ exists because sediments can contain significant amounts of inorganic
142 nitrogen that includes ammonium adsorbed onto clay minerals (Müller, 1977; Schubert & Calvert,
143 2001; Stevenson & Dhariwal, 1959). By removing organic nitrogen from the bulk sediment with
144 a KOB_r-KOH solution, it is possible to measure the amount of bound inorganic nitrogen and its
145 isotopic composition (Knies et al., 2007; Schubert and Calvert, 2001). The $\delta^{15}\text{N}$ of the organic
146 nitrogen is then obtained by calculation using the inorganic signal and the bulk $\delta^{15}\text{N}$ in a mass
147 balance equation. This correction removes the potential bias of inorganic nitrogen. Bulk $\delta^{15}\text{N}$ can
148 be altered during burial and early diagenesis, particularly outside of continental margin (Robinson
149 et al., 2012). While it is not possible to unilaterally reject the potential influence of alteration, there
150 is no reasons to suspect large and/or variable alteration of the signal through time as our site was
151 at shallow depth (10 to 30 m) throughout the Holocene (Bauch et al., 2001b). Finally, since our
152 core was located near the coast for the Holocene, we hypothesise that the surface water was never
153 completely limited in nitrate during that period. This is supported by the current setting, were
154 nitrate are not totally used during summer (Fig. 2). It is important to note that the present distance
155 between the core and the coastline is at its maximum for the Holocene, and thus we can suspect
156 that the quantity of nutrient reaching that position is therefore at its minimum for the Holocene.
157 The last factor, beside N-utilization, that could influence our $\delta^{15}\text{N}$ record is the initial signature of
158 the organic material, which can be modified depending on the source of nitrogen (e.g., terrestrial
159 vs marine). Thus, we interpret our $\delta^{15}\text{N}$ record as variation in the ratio of terrestrial to marine
160 organic matter, and/or in a change in N-utilization depending on the information gathered from
161 other proxy.

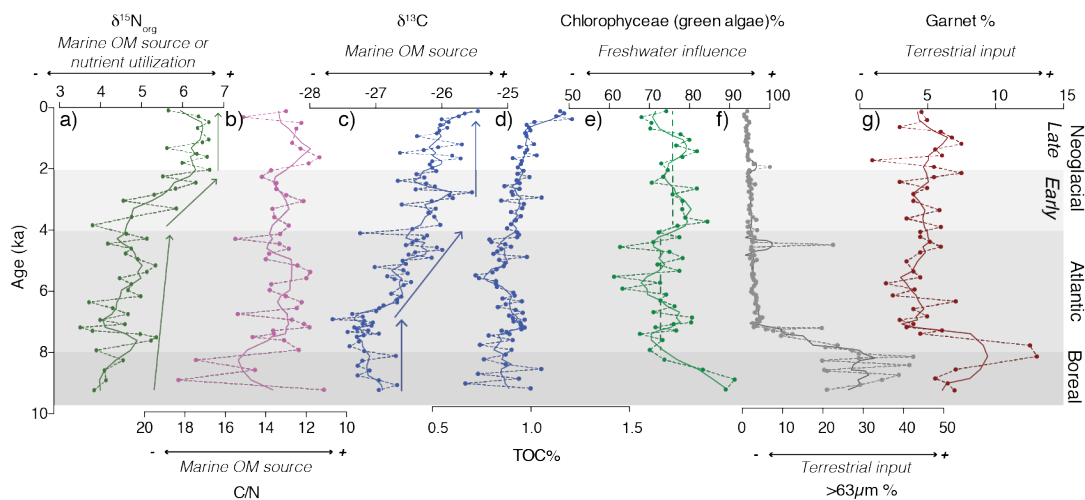
162 Nitrogen content and isotope ratio for both bulk and inorganic nitrogen were analyzed by
163 elemental analyser isotope ratio mass spectrometer (EA-IRMS). The precision for treated and
164 untreated samples was better than ± 0.2 ‰. Organic nitrogen isotope was calculated by subtracting
165 the inorganic value from the bulk isotopic composition (e.g., Knies et al., 2007). The age model
166 and the other proxies for core PM9462 were originally described by Bauch et al. (2001a, 2001b).

167

168 **4. Results**

169 Three distinct periods characterized core PM9462. The bottom of the core (> 8 ka; Boreal
170 period) has a high proportion of terrestrial markers like sand (40%) and garnet (13%), as well as
171 typical terrestrial signatures of $\delta^{13}\text{C}_{\text{org}}$ (-27 ‰) and C:N (>15) (Fig. 3). Sand, C/N ratio and total
172 organic carbon notably show a high degree of variability. This part also has the highest proportion
173 of freshwater algae (>70 to 90 % of total algae content). The $\delta^{15}\text{N}$ of organic nitrogen is slightly
174 higher than 4 ‰. The regime transitions from heavily dominated by terrestrial-markers during the
175 Boreal to more marine-influenced conditions in the Atlantic period (8 to 4 ka); the proportion of
176 sand and garnet decreases dramatically right at the transition and decrease slowly without much
177 variability (sand) or stays constant on average but with a high variability (garnet). The $\delta^{13}\text{C}_{\text{org}}$ starts
178 increasing gradually toward -26 ‰ about 1 ka after the transition, while the C:N ratio drops rapidly
179 to ~ 13 and stays constant on average but with a high variability. Moreover, we observe the lowest
180 proportion of freshwater algae (~ 70 %) and a gradual increase in the isotopic composition of
181 organic nitrogen (Fig. 3). The third period (4 to 0 ka; Neoglacial period) is characterized by
182 relatively constant terrestrial vs marine markers (sand, garnet, $\delta^{13}\text{C}_{\text{org}}$, C:N). However, we could
183 subdivide this period in two parts (early and late) as there is a sharp increase in the $\delta^{15}\text{N}$ around 4
184 ka and a stabilization (~ 6.5 ‰) at around 2 ka (Fig. 3). The Neoglacial is also characterized by

185 statistically significant higher freshwater algae (average = 76.19% ± 0.97, $P < 0.05$; Mann-Whitney
 186 test performed with ©Prism7.0d) than the Atlantic period (average = 72.84% ± 1.05). The
 187 freshwater algae record is characterized by high variability in the Atlantic and Neoglacial periods.
 188



189
 190 Fig 3. Sedimentary proxy in core PM9462 in function of the age model: **a)** $\delta^{15}\text{N}$ of organic nitrogen (green,
 191 in ‰), **b)** carbon to nitrogen ratio (pink), **c)** $\delta^{13}\text{C}$ of the organic carbon (blue, in ‰), **d)** total organic carbon
 192 (blue, in ‰), **e)** the proportion of green algae (green, in ‰), **f)** the proportion of sand (grey, in ‰) and **g)** the
 193 proportion of garnet (red, in ‰). A 4-neighbors, 2nd order smoothing was applied to all dataset to see the
 194 general trend (solid lines).

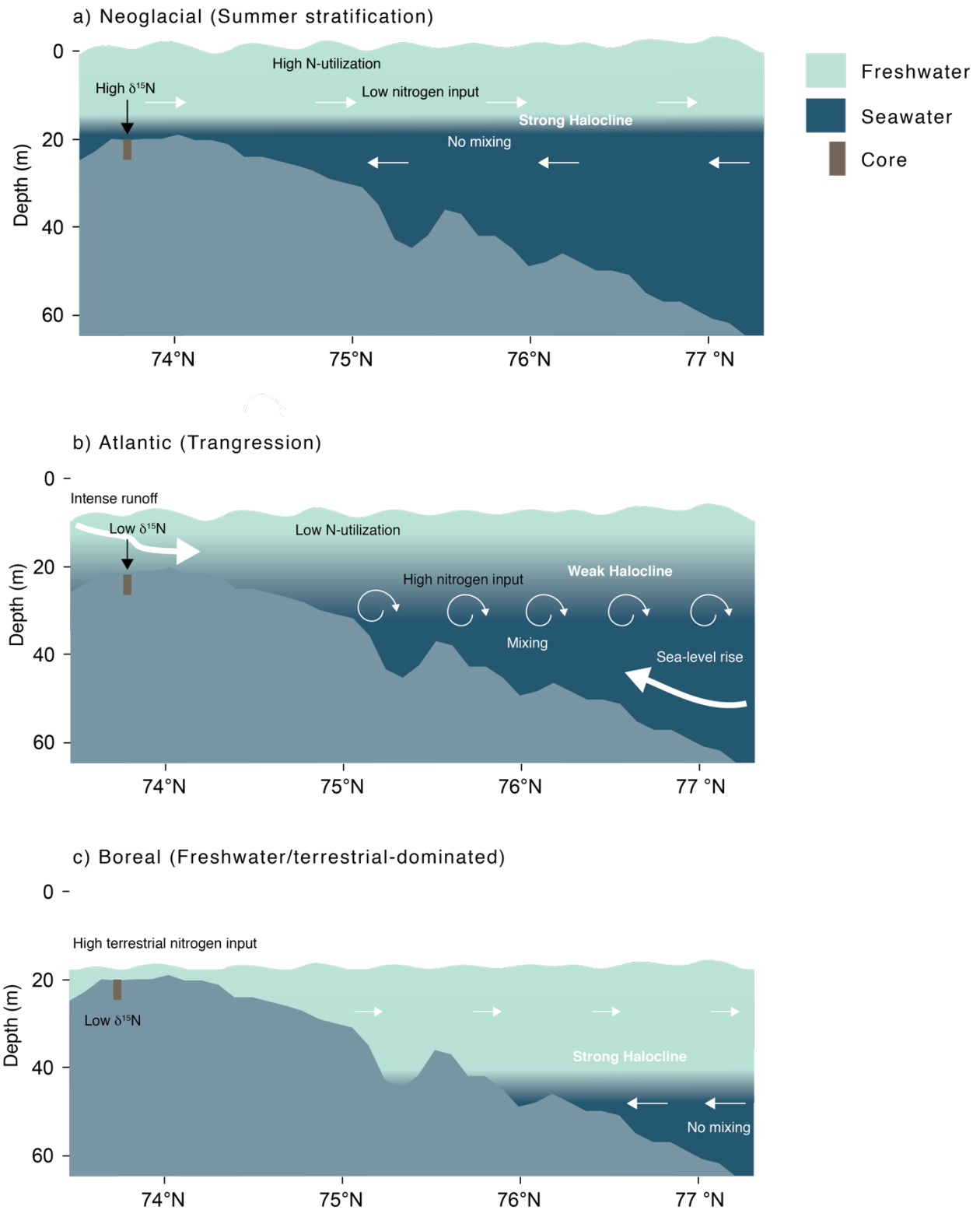
195
 196 **5. Enhanced nitrogen utilization during the Neoglacial**

197 The proxy data from core PM9462 recorded a mixture of two signals: (1) the shift from
 198 terrestrial dominated input to a more marine-influenced organic matter input; (2) change in nutrient
 199 utilization due to change in the water column stratification. The first part of the story is well
 200 documented over the Laptev and Kara Seas (e.g., Bauch et al., 2001a, 1999; Boucsein et al., 2002;
 201 Stein et al., 2004, 2001, 1999; Stein and Fahl, 2000). With the initial transgression of the Laptev
 202 Sea, a clear transition during the Atlantic period occurred where: (1) most of the geologic marker

203 of detritic input decreased; (2) the freshwater markers decreased; (3) the proportion of marine
204 organic matter increased (Fig. 3). The latter signal is primarily registered in the $\delta^{13}\text{C}_{\text{org}}$ record with
205 a trend towards gradually heavier values since c. 7 ka, which is consistent with other geochemical
206 proxies (e.g., Stein et al., 1999). The $\delta^{15}\text{N}_{\text{org}}$ remained largely constant (4 to 5‰) during the Boreal
207 and Atlantic period, highlighting the gradual increase in marine-dominated organic matter from
208 the Boreal to the Atlantic (e.g., Stein et al., 2001). This transition to heavier values might be
209 partially masked by a low N-utilization facilitated by the absence of a strong pycnocline during
210 summer, allowing the mixing of surface water with nutrient rich Atlantic-derived waters
211 (Thibodeau et al., 2017a). The masking effect of N-utilization might explain the small discrepancy
212 between the transition in the early part of the Atlantic periods between $\delta^{15}\text{N}$ and the other
213 marine/terrestrial markers (Fig 3). The time between 5 and 8 ka is characterized not only by a
214 constant sea-level rise but also by intense river runoff. That riverine water should have promoted
215 a higher rate of freshwater algae input. However, at our study site we recorded the lowermost
216 amount of these algae during the entire Holocene. A possible explanation for this discrepancy
217 could be that the surface water was slightly saltier than during the Neoglacial. We explain this by
218 suggesting that the intense river runoff combined with the sea-level rise could have created a
219 relatively unstable water column and promoted mixing of surface water with deeper water (Fig. 4).
220 This assumption would be coherent with the irregular sedimentation regime observed during the
221 5-8 ka period, which was attributed to sea-level rise (Bauch et al., 2001a). This is supported by
222 $\delta^{18}\text{O}$ values from bivalve shells, which found the highest summer salinity value of the Holocene
223 at around 4 ka (Mueller-Lupp et al., 2004). On the other hand, diatoms reconstruction suggest that
224 the Neoglacial was slightly more saline (by about 0.3 psu) compared to the Atlantic period

225 (Polyakova et al., 2005). Irrespective of the proxy used, the difference in salinity between the
226 Atlantic and the Neoglacial seems to have been minor.

227 The transition to the Neoglacial is characterized by a sharp rise in $\delta^{15}\text{N}_{\text{org}}$ during the early part
228 of the period followed by its stabilization at around 2.5 ka. Since the proportions of marine and
229 terrigenous organic matter remained constant during the whole Neoglacial, the sharp rise in the
230 $\delta^{15}\text{N}_{\text{org}}$ record around 4 ka is caused by an increase in the nutrient limitation rather than a change
231 of source of nitrogen. The reason for this sharp increase is likely due to the establishment of a
232 strong summer stratification after sea-level rise came to a standstill and thus, enhanced nutrient
233 utilization in the uppermost water masses in the Laptev Sea shelf (Fig. 4).



234

235 Fig 4. Schematic of our conceptual model for the a) Neoglacial, b) Atlantic and c) Boreal period

236 oceanography of the Laptev Sea shelf. The sediment core PM9462 is represented by the brown rectangle.

237 The **c)** Boreal period was characterized by a high amount of freshwater and high terrestrial input (low $\delta^{15}\text{N}$)
238 due to the proximity of the core to the river mouth. The high input of nutrient was probably also causing
239 low nutrient utilization (low $\delta^{15}\text{N}$). Our coring site was dominated by freshwater. The **b)** Atlantic period
240 was dominated by the transgression, sea-level rises and the gradual increasing influence of marine water at
241 our coring site throughout the period. The gradual increase in marine organic matter drove the slight
242 increase in $\delta^{15}\text{N}$ as the strong mixing due to the transgression probably kept the nutrient utilization low (low
243 $\delta^{15}\text{N}$). Summer stratification was established only during the **a)** Neoglacial, after the sea-level reached a
244 standstill, the strong halocline and decreased riverine input reduced the nitrogen input and increased the
245 nutrient utilization (high $\delta^{15}\text{N}$).

246

247 **6. Evolution of the Laptev Sea stratification and sea-ice export by the Transpolar Drift (TD)** 248 **system during the Holocene**

249 The single most important factor that might control Arctic sea-ice production during the
250 Holocene is the position and the size of large polynyas off Siberia, from which the Laptev Sea is
251 considered the most important being closest to where the TD originates (Krumpfen et al., 2016;
252 Reimnitz et al., 1994; Zakharov, 1966). While changes in sea-ice coverage varied throughout the
253 Holocene (Hörner et al., 2016), the underlying mechanism driving the variability throughout the
254 Holocene is still equivocal. Increase in sea-level during the Holocene should be suspected to have
255 an influence on the configuration on the Laptev Sea ice factory. However, no clear evidence was
256 available to reconstruct the variability of this configuration. Here, we use our reconstruction of the
257 summer stratification as a proxy of favourable condition for sea-ice production in the Laptev Sea
258 and compare the result with a Holocene record of sea-ice algae production from the Laptev Sea
259 and paleoceanographic data from the Atlantic end of the TD (Fig. 5).

260

261 6.1 *Boreal and Atlantic (10 to ~ 4 ka)*

262 The postglacial sea-level in the Laptev Sea rose by about 40 m during the Holocene
263 transgression (Bauch et al., 2001b). The data suggest a relatively low nitrate-utilization and that
264 most organic matter originated from land, which is consistent with previous findings using organic
265 geochemical proxies (e.g., Boucsein et al., 2002; Fahl and Stein, 1999; Stein et al., 1999). The
266 latter is also supported by our first-hand approximation of the proportion of terrestrial organic
267 matter based on the $\delta^{13}\text{C}_{\text{org}}$, which suggest that about 87 % of the total organic matter was of
268 terrigenous origin (SOM). That assumption is coherent with the oldest part of the core where the
269 $\delta^{15}\text{N}$ value is similar to the $\delta^{15}\text{N}$ value of particulate organic matter measured in the Lena River
270 (4.6 ‰) (McClelland et al., 2016), corroborating the terrestrial origin of most of the organic matter
271 during this period. During this period the water column was well-mixed with advection of nutrient-
272 rich bottom water on the shelf due to the rapid sea-level rise (8 to 13 $\text{mm}\cdot\text{yr}^{-1}$; Bauch et al., 2001b,
273 2001a). Unstable conditions were also observed in Fram Strait, with a weakly stratified water
274 column and a strong influence of Atlantic water (Werner et al., 2016). During this relatively warm
275 period, very low sea-ice algae production was reconstructed in Fram Strait and on the Greenland
276 and Icelandic shelves based on IP_{25} (Fig 5; Cabedo-Sanz et al., 2016; Müller et al., 2012; Werner
277 et al., 2013). Moreover, the presence of warm Atlantic water was observed at the Reykjanes Ridge,
278 suggesting a weak East Greenland current and a relatively northward positioning of the sub-Arctic
279 front (Moros et al., 2012; Perner et al., 2017). Furthermore, a thin mixed-layer was observed in the
280 Nordic Sea during this period, suggesting a weak import of surface freshwater from the Arctic
281 (Thibodeau et al., 2017b). During the Holocene, modern sea-ice condition over the central Arctic,
282 with a perennial sea-ice cover, was established around 5-8 ka (Cronin et al., 2010; Fahl and Stein,
283 2012). Thus, during this period, the Laptev Sea was characterized by a mixed water column and

284 conditions unfavorable to intense sea-ice formation. This is illustrated by the slight increase of sea-
285 ice algae production at the beginning of the Atlantic period, which become more important at
286 around 6.5 ka but stays around 50% of the modern-day value (Fig. 5b). Coincidentally, sea-ice
287 export through Fram Strait was minimal, as suggested by the low IRD, and upper-ocean
288 stratification was high in the Nordic Sea, suggesting a thin surface mixed-layer due to weak
289 freshwater export from the Arctic (Fig. 5e, h).

290

291 *6.2 Early Neoglacial (~ 4 to 2 ka)*

292 After the sea-level reached its highstand at around 4-5 ka (Bauch et al., 2001a, 2001b), the
293 condition became more stable in the Laptev Sea and a transition phase from the pre-4 ka unstable
294 conditions toward the modern, highly-stratified, oceanographic setting commenced (Fig. 5a). This
295 transition phase was characterized by an increase in nutrient utilization due to the progressive
296 stabilization of the water column and river runoff as suggested by the consistency of most of the
297 proxy data in this part of the core (i.e., no change in the marine to terrestrial ratio of organic matter
298 input; Fig. 3). The ongoing stabilization of the water column here provided increasingly favourable
299 conditions for the formation of polynyas and pack ice. Interestingly, there is no synchronous
300 response in the sea-ice algae production over the Laptev Sea during this period (Fig. 5b). The
301 1800-year cycle identified in the IP₂₅ record indicates that, at this timescale, there is a strong
302 linkages between sea-ice formation and atmospheric processes like the Arctic and North Atlantic
303 oscillations in the Laptev Sea (Hörner et al., 2016). A similar cycle have been identified in
304 reconstruction of Arctic sea-ice drift during the Holocene (Darby et al., 2012). During the same
305 period, sea-ice cover continuously increased in the high Arctic (e.g., Xiao et al., 2015), Chukchi
306 Sea (Stein et al., 2017), Baffin Bay (e.g., Kolling et al., 2018), Fram Strait (e.g., Werner et al.,

307 2013) and over the Icelandic shelf (Cabedo-Sanz et al., 2016) but only slightly over the Greenland
308 shelf (Kolling et al., 2017; Müller et al., 2012). While climatic conditions became more favourable
309 for in-situ sea-ice formation in the Arctic and marginal seas, the three-fold increase in IRD in Fram
310 Strait (Werner et al., 2013) suggest a synchronous enhanced sea-ice export from the Arctic (Fig.
311 5e). Interestingly, the water column in Fram Strait also transitioned to a strongly stratified water
312 column at around 3 ka as indicated by the difference between the $\delta^{13}\text{C}$ values of *Neogloboquadrina*
313 *pachyderma* sinistral (NPs) and *Turborotalita quinqueloba* (Fig. 5f), with much cooler water at
314 the surface as evidenced by the abundance of NPs (Fig. 5e). That change in stratification was also
315 observed in the Nordic Seas, where the mixed-layer depth increased through this period,
316 suggesting increased flux of freshwater from the Arctic (Thibodeau et al., 2017b). Much cooler
317 surface water was observed over the Icelandic shelf and the Reykjanes Ridge linked with
318 freshwater input and a greater influence of the sub-Arctic front (Cabedo-Sanz et al., 2016; Moros
319 et al., 2012; Perner et al., 2017).

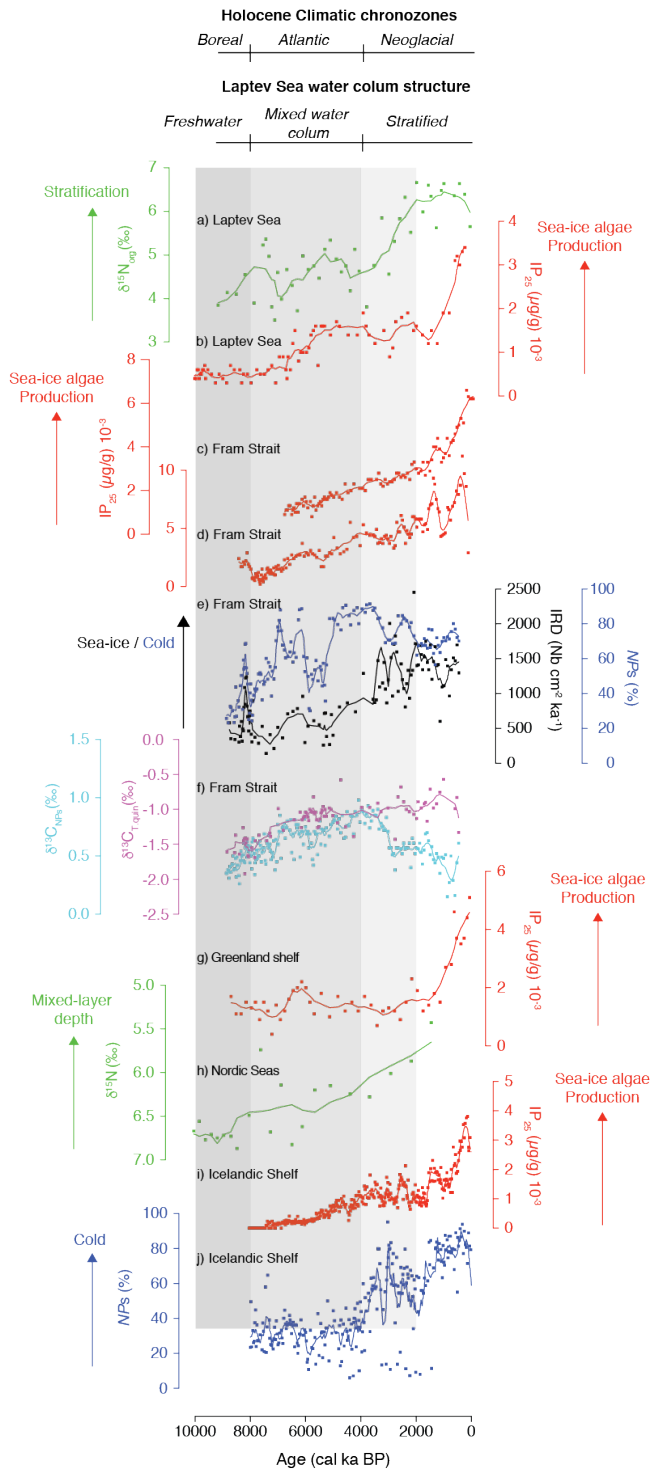
320

321 6.3 Late Neoglacial (2 ka to Recent)

322 The complete stabilization of the modern summer stratification of the Laptev Sea was reached
323 at 2 ka (Fig. 5a). We believe that it is also the onset of the present-day configuration of the so
324 called “sea-ice factory” of the Laptev Sea. This configuration allowed the increase in sea-ice cover
325 suggested by the increase in sea-ice algae production (Fig. 5b). However, the increase was not
326 simultaneous probably because of the decrease observed in the 1800-year cycle in sea-ice cover
327 that is driving most of the short-term sea-ice algae production variability (Hörner et al., 2016).
328 Temperature reconstruction during this period suggests a local trend with warmer surface water
329 and more stratified upper-ocean structure in Fram Strait while the Nordic Seas and the Icelandic

330 shelf are characterized by cooler surface water (Cabedo-Sanz et al., 2016; Thibodeau et al.,
331 2017b; Werner et al., 2013). Sea-ice algae production is generally increasing at all sites (Fram
332 Strait, Greenland and Icelandic shelves), culminating at the end of the record when sea-ice margin
333 reached its southern location (Perner et al., 2017) (Fig. 5). In this part of the record the IRD
334 suggests a constant export of sea-ice from the Arctic to Fram Strait (Fig. 5e). Moreover, a shift in
335 the mineral source region from Arctic to Fjord at around 1.2 ka in core from East Greenland shelf
336 might be related to increased outflow from Fjords and is correlated with glacier advance in
337 Greenland indicating a widespread increase in sea-ice production (Kolling et al., 2017; Solomina
338 et al., 2015).

339



340

341 Fig 5. Reconstruction of **a)** stratification in the Laptev Sea based on $\delta^{15}\text{N}$, **b)** sea-ice algae production in
 342 the Laptev Sea based on IP_{25} (Hörner et al., 2016), **c)** and **d)** sea-ice algae production in Fram Strait (MSM5-
 343 723-2 and 712-2) based on IP_{25} (Müller et al., 2012; Werner et al., 2013), **e)** sea-ice import and subsurface

344 temperature in Fram Strait (MSM5-712-2) based on ice-rafted debris and polar planktic foraminifera
345 *Neogloboquadrina pachyderma* sinistral (NPs) respectively (Werner et al., 2013), **f**) stratification of Fram
346 strait (MSM5-712-2) based on $\delta^{13}\text{C}$ of *Neogloboquadrina pachyderma* sinistral and *Turborotalita*
347 *quinqueloba* (Werner et al., 2013), **g**) sea-ice algae production over the Greenland shelf (PS2641-4) based
348 on IP₂₅ (Müller et al., 2012), **h**) stratification in the Nordic Seas (PS1243) based on $\delta^{15}\text{N}$ (Thibodeau et al.,
349 2017b), **i**) sea-ice algae production over the Icelandic shelf (MD99-2269) based on IP₂₅, (Cabedo-Sanz et
350 al., 2016), **j**) subsurface temperature over the Greenland shelf (MD99-2269) based on polar planktic
351 foraminifera *Neogloboquadrina pachyderma* sinistral (Cabedo-Sanz et al., 2016). A 4-neighbors, 2nd order
352 smoothing was applied to all dataset to see the general trend (solid lines).

353

354

355 **7. Paleoclimatic Implications**

356 Our results highlight the fact that favorable conditions for sea-ice formation in the Laptev Sea
357 after 2 ka are concomitant to enhanced export of sea-ice via Fram Strait and the installment of
358 modern-like conditions along the TD up to the central Nordic Seas. This also implies a change in
359 the Arctic atmospheric circulation system after the mid-Holocene as it drives the TD. Thus, we
360 suggest that the establishment of a stable water column structure in the Laptev Sea, after the
361 Holocene transgression, had a significant impact on the sea-ice dynamic over the Arctic and on
362 the freshwater export via Fram Strait. This increase in freshwater export probably contributed to
363 regulate climate during the last 2 000 years through its impact on Arctic heat budget and on polar
364 North Atlantic stratification. While more work is needed to disentangle the exact drivers of sea-
365 ice variability throughout the Holocene, we show here that the onset of coastal Arctic sea-ice
366 factory probably played a role, along solar activity, in the production of sea-ice and its export

367 toward the North Atlantic. This needs to be considered when trying to reconstruct Arctic Ocean
368 sea-ice drift and coverage based on paleo-data and/or modelling (e.g., Funder et al., 2011).

369

370 **Acknowledgements**

371 Original data are available in the online supplementary material. Part of this work was funded by
372 DFG through individual research grant awarded to BT (TH1933/1-1) and the Stephen S.F. Hui
373 Trust Fund. JK is supported by the Norwegian Research Council through its Centres of Excellence
374 funding scheme (grant 223259) and Petromaks2 program (grant 255150). The study contributes to
375 the Russian-German "Laptev Sea System" through CATS. We are thankful to Ruediger Stein and
376 one anonymous reviewer for their very constructive comments. We also thank Mandy Wing Kwan
377 So for her assistance with figure 1 and 4 and Kayi Chan for her comments on the manuscript and
378 U. Struck for analytical support.

379

380 **References**

- 381 Altabet, M.A., Francois, R., 1994. Sedimentary nitrogen isotopic ratio as a recorder for surface
382 ocean nitrate utilization. *Global Biogeochem. Cycles* 8, 103–116. doi:10.1029/93GB03396
- 383 Bauch, D., Hölemann, J., Dmitrenko, I., Janout, M., Nikulina, A., Kirillov, S., Krumpfen, T.,
384 Kassens, H., Timokhov, L., 2012. Impact of Siberian coastal polynyas on shelf-derived
385 Arctic Ocean halocline waters. *J. Geophys. Res. Ocean.* 117. doi:10.1029/2011JC007282
- 386 Bauch, H.A., Kassens, H., Erlenkeuser, H., Grootes, P.M., Thiede, J., 1999. Depositional
387 environment of the Laptev Sea (Arctic Siberia) during the Holocene. *Boreas* 28, 194–204.
- 388 Bauch, H.A., Kassens, H., Naidina, O.D., Kunz-Pirrung, M., Thiede, J., 2001a. Composition and
389 flux of Holocene sediments on the eastern Laptev Sea Shelf, Arctic Siberia. *Quat. Res.* 55,
390 344–351. doi:10.1006/qres.2000.2223
- 391 Bauch, H.A., Mueller-Lupp, T., Taldenkova, E., Spielhagen, R.F., Kassens, H., Grootes, P.M.,
392 Thiede, J., Heinemeier, J., Petryashov, V. V., 2001b. Chronology of the holocene
393 transgression at the north siberian margin. *Glob. Planet. Change* 31, 125–139.
394 doi:10.1016/S0921-8181(01)00116-3
- 395 Belkin, I.M., Levitus, S., Antonov, J., Malmberg, S.-A., 1998. “Great Salinity Anomalies” in the
396 North Atlantic. *Prog. Oceanogr.* 41, 1–68. doi:10.1016/S0079-6611(98)00015-9
- 397 Bond, G., Kromer, B., Beer, J., Muscheler, R., Evans, M.N., Showers, W., Hoffmann, S., Lotti-
398 Bond, R., Hajdas, I., Bonani, G., 2001. Persistent solar influence on north atlantic climate
399 during the Holocene. *Science (80-)*. 294, 2130–2136. doi:10.1126/science.1065680
- 400 Bond, G., Showers, W., Cheseby, M., Lotti, R., Almasi, P., DeMenocal, P., Priore, P., Cullen,
401 H., Hajdas, I., Bonani, G., 1997. A pervasive millennial-scale cycle in North Atlantic
402 Holocene and glacial climates. *Science (80-)*. 278, 1257–1266.
403 doi:10.1126/science.278.5341.1257
- 404 Boucsein, B., Knies, J., Stein, R., 2002. Organic matter deposition along the Kara and Laptev
405 Seas continental margin (eastern Arctic Ocean) during last deglaciation and Holocene:
406 evidence from organic–geochemical and petrographical data. *Mar. Geol.* 183, 67–87.
407 doi:10.1016/S0025-3227(01)00249-3
- 408 Cabedo-Sanz, P., Belt, S.T., Jennings, A.E., Andrews, J.T., Geirsdóttir, Á., 2016. Variability in
409 drift ice export from the Arctic Ocean to the North Icelandic Shelf over the last 8000 years:
410 A multi-proxy evaluation. *Quat. Sci. Rev.* 146, 99–115.
411 doi:10.1016/j.quascirev.2016.06.012
- 412 Comiso, J.C., Parkinson, C.L., Gersten, R., Stock, L., 2008. Accelerated decline in the Arctic sea
413 ice cover. *Geophys. Res. Lett.* 35. doi:10.1029/2007GL031972
- 414 Cronin, T.M., Gemery, L., Briggs, W.M., Jakobsson, M., Polyak, L., Brouwers, E.M., 2010.
415 Quaternary Sea-ice history in the Arctic Ocean based on a new Ostracode sea-ice proxy.
416 *Quat. Sci. Rev.* 29, 3415–3429. doi:10.1016/j.quascirev.2010.05.024
- 417 Curry, R., 2005. Dilution of the Northern North Atlantic Ocean in Recent Decades. *Science*
418 (80-). 308, 1772–1774. doi:10.1126/science.1109477
- 419 Darby, D.A., Ortiz, J.D., Grosch, C.E., Lund, S.P., 2012. 1,500-year cycle in the Arctic
420 Oscillation identified in Holocene Arctic sea-ice drift. *Nat. Geosci.* 5, 897–900.
421 doi:10.1038/ngeo1629
- 422 Dickson, R.R., Meincke, J., Malmberg, S.-A., Lee, A.J., 1988. The “great salinity anomaly” in
423 the Northern North Atlantic 1968–1982. *Prog. Oceanogr.* 20, 103–151. doi:10.1016/0079-
424 6611(88)90049-3

425 Dmitrenko, I., Kirillov, S., Eicken, H., Markova, N., 2005. Wind-driven summer surface
426 hydrography of the eastern Siberian shelf. *Geophys. Res. Lett.* 32.
427 doi:10.1029/2005GL023022

428 Dmitrenko, I., Kirillov, S., Tremblay, L.B., 2008. The long-term and interannual variability of
429 summer fresh water storage over the eastern Siberian shelf: Implication for climatic change.
430 *J. Geophys. Res.* 113. doi:10.1029/2007JC004304

431 Dmitrenko, I.A., Kirillov, S.A., Bloshkina, E., Lenn, Y.D., 2012. Tide-induced vertical mixing in
432 the Laptev Sea coastal polynya. *J. Geophys. Res. Ocean.* 117. doi:10.1029/2011JC006966

433 Dmitrenko, I.A., Kirillov, S.A., Krumpen, T., Makhotin, M., Povl Abrahamsen, E., Willmes, S.,
434 Bloshkina, E., Hölemann, J.A., Kassens, H., Wegner, C., 2010. Wind-driven diversion of
435 summer river runoff preconditions the Laptev Sea coastal polynya hydrography: Evidence
436 from summer-to-winter hydrographic records of 2007-2009. *Cont. Shelf Res.* 30, 1656–
437 1664. doi:10.1016/j.csr.2010.06.012

438 Dmitrenko, I.A., Kirillov, S.A., Tremblay, L.B., Bauch, D., Willmes, S., 2009. Sea-ice
439 production over the Laptev Sea shelf inferred from historical summer-to-winter
440 hydrographic observations of 1960s–1990s. *Geophys. Res. Lett.* 36, L13605.
441 doi:10.1029/2009GL038775

442 Fahl, K., Stein, R., 2012. Modern seasonal variability and deglacial/Holocene change of central
443 Arctic Ocean sea-ice cover: New insights from biomarker proxy records. *Earth Planet. Sci.*
444 *Lett.* 351–352, 123–133. doi:10.1016/j.epsl.2012.07.009

445 Fahl, K., Stein, R., 1999. Biomarkers as organic-carbon-source and environmental indicators in
446 the Late Quaternary Arctic Ocean: problems and perspectives. *Mar. Chem.* 63, 293–309.
447 doi:10.1016/S0304-4203(98)00068-1

448 Funder, S., Goosse, H., Jepsen, H., Kaas, E., Kjaer, K.H., Korsgaard, N.J., Larsen, N.K.,
449 Linderson, H., Lysa, A., Moller, P., Olsen, J., Willerslev, E., 2011. A 10,000-Year Record
450 of Arctic Ocean Sea-Ice Variability--View from the Beach. *Science* (80-). 333, 747–750.
451 doi:10.1126/science.1202760

452 Galbraith, E.D., Sigman, D.M., Robinson, R.S., Pedersen, T.F., 2008. Nitrogen in Past Marine
453 Environments, Nitrogen in the Marine Environment. doi:10.1016/B978-0-12-372522-
454 6.00034-7

455 Hörner, T., Stein, R., Fahl, K., Birgel, D., 2016. Post-glacial variability of sea ice cover, river
456 run-off and biological production in the western Laptev Sea (Arctic Ocean) – A high-
457 resolution biomarker study. *Quat. Sci. Rev.* 143, 133–149.
458 doi:10.1016/j.quascirev.2016.04.011

459 Ionita, M., Scholz, P., Lohmann, G., Dima, M., Prange, M., 2016. Linkages between atmospheric
460 blocking, sea ice export through Fram Strait and the Atlantic Meridional Overturning
461 Circulation. *Sci. Rep.* 6. doi:10.1038/srep32881

462 Kattner, G., Lobbes, J. M., Fitznar, H. P., Engbrodt, R., Nöthig, E.-M.M., Lara, R. J., 1999.
463 Tracing dissolved organic substances and nutrients from the Lena River through Laptev Sea
464 (Arctic). *Mar. Chem.* 65, 25–39. doi:10.1016/S0304-4203(99)00008-0

465 Knies, J., Brookes, S., Schubert, C.J., 2007. Re-assessing the nitrogen signal in continental
466 margin sediments: New insights from the high northern latitudes. *Earth Planet. Sci. Lett.*
467 253, 471–484. doi:10.1016/j.epsl.2006.11.008

468 Kolling, H.M., Stein, R., Fahl, K., Perner, K., Moros, M., 2018. New insights into sea ice
469 changes over the past 2 . 2 kyr in Disko Bugt , West Greenland. *arktos* 4, 11.
470 doi:10.1007/s41063-018-0045-z

471 Kolling, H.M., Stein, R., Fahl, K., Perner, K., Moros, M., 2017. Short-term variability in late
472 Holocene sea ice cover on the East Greenland Shelf and its driving mechanisms.
473 *Palaeogeogr. Palaeoclimatol. Palaeoecol.* 485, 336–350. doi:10.1016/j.palaeo.2017.06.024
474 Krumpfen, T., Gerdes, R., Haas, C., Hendricks, S., Herber, A., Selyuzhenok, V., Smedsrud, L.,
475 Spreen, G., 2016. Recent summer sea ice thickness surveys in Fram Strait and associated ice
476 volume fluxes. *Cryosphere* 10, 523–534. doi:10.5194/tc-10-523-2016
477 Krumpfen, T., Holemann, J. a., Willmes, S., Morales Maqueda, M. a., Busche, T., Dmitrenko, I.
478 a, Gerdes, R., Haas, C., Heinemann, G., Hendricks, S., Kassens, H., Rabenstein, L.,
479 Schröder, D., 2011. Sea ice production and water mass modification in the eastern Laptev
480 Sea. *J. Geophys. Res. C Ocean.* 116, 1–17. doi:10.1029/2010JC006545
481 Krumpfen, T., Janout, M., Hodges, K.I., Gerdes, R., Girard-Ardhuin, F., Hölemann, J.A.,
482 Willmes, S., 2013. Variability and trends in Laptev Sea ice outflow between 1992–2011.
483 *Cryosph.* 7, 349–363. doi:10.5194/tc-7-349-2013
484 Levitus, S., Antonov, J.I., Baranova, O.K., Boyer, T.P., Coleman, C.L., Garcia, H.E., Grodsky,
485 A.I., Johnson, D.R., Locarnini, R.A., Mishonov, A. V, Reagan, J.R., Sazama, C.L., Seidov,
486 D., Smolyar, I., Yarosh, E.S., Zweng, M.M., 2013. The World Ocean Database. *Data Sci. J.*
487 12, WDS229-WDS234. doi:10.2481/dsj.WDS-041
488 Manabe, S., Stouffer, R.J., 1980. Sensitivity of a global climate model to an increase of CO₂
489 concentration in the atmosphere. *J. Geophys. Res.* 85, 5529–5554.
490 doi:10.1029/JC085iC10p05529
491 McClelland, J.W., Holmes, R.M., Peterson, B.J., Raymond, P.A., Striegl, R.G., Zhulidov, A. V.,
492 Zimov, S.A., Zimov, N., Tank, S.E., Spencer, R.G.M., Staples, R., Gurtovaya, T.Y., Griffin,
493 C.G., 2016. Particulate organic carbon and nitrogen export from major Arctic rivers. *Global*
494 *Biogeochem. Cycles* 30, 629–643. doi:10.1002/2015GB005351
495 Moros, M., Jansen, E., Oppo, D.W., Giraudeau, J., Kuijpers, A., 2012. Reconstruction of the
496 late-Holocene changes in the Sub-Arctic Front position at the Reykjanes Ridge, north
497 Atlantic. *The Holocene* 22, 877–886. doi:10.1177/0959683611434224
498 Mueller-Lupp, T., Bauch, H.A., Erlenkeuser, H., 2004. Holocene hydrographical changes of the
499 eastern Laptev Sea (Siberian Arctic) recorded in $\delta^{18}\text{O}$ profiles of bivalve shells. *Quat. Res.*
500 61, 32–41. doi:10.1016/j.yqres.2003.09.003
501 Müller, J., Werner, K., Stein, R., Fahl, K., Moros, M., Jansen, E., 2012. Holocene cooling
502 culminates in sea ice oscillations in Fram Strait. *Quat. Sci. Rev.* 47, 1–14.
503 doi:10.1016/j.quascirev.2012.04.024
504 Müller, P.J., 1977. C/N ratios in Pacific deep-sea sediments: Effect of inorganic ammonium and
505 organic nitrogen compounds sorbed by clays. *Geochim. Cosmochim. Acta* 41, 765–776.
506 doi:10.1016/0016-7037(77)90047-3
507 Perner, K., Moros, M., Jansen, E., Kuijpers, A., Troelstra, S.R., Prins, M.A., 2017. Subarctic
508 Front migration at the Reykjanes Ridge during the mid- to late Holocene: evidence from
509 planktic foraminifera. *Boreas*. doi:10.1111/bor.12263
510 Perovich, D.K., Richter-Menge, J.A., 2009. Loss of Sea Ice in the Arctic. *Ann. Rev. Mar. Sci.* 1,
511 417–441. doi:10.1146/annurev.marine.010908.163805
512 Polyakova, Y.I., Bauch, H.A., Klyuvitkina, T.S., 2005. Early to middle Holocene changes in
513 Laptev Sea water masses deduced from diatom and aquatic palynomorph assemblages.
514 *Glob. Planet. Change* 48, 208–222. doi:10.1016/j.gloplacha.2004.12.014
515 Reimnitz, E., Dethleff, D., Nürnberg, D., 1994. Contrasts in Arctic shelf sea-ice regimes and
516 some implications: Beaufort Sea versus Laptev Sea. *Mar. Geol.* 119, 215–225.

517 doi:10.1016/0025-3227(94)90182-1
518 Riethdorf, J.R., Thibodeau, B., Ikehara, M., Nürnberg, D., Max, L., Tiedemann, R., Yokoyama,
519 Y., 2016. Surface nitrate utilization in the Bering sea since 180 kA BP: Insight from
520 sedimentary nitrogen isotopes. *Deep. Res. Part II Top. Stud. Oceanogr.* 125–126, 163–176.
521 doi:10.1016/j.dsr2.2015.03.007
522 Rigor, I., Colony, R., 1997. Sea-ice production and transport of pollutants in the Laptev Sea,
523 1979–1993. *Sci. Total Environ.* 202, 89–110. doi:https://doi.org/10.1016/S0048-
524 9697(97)00107-1
525 Robinson, R.S., Brunelle, B.G., Sigman, D.M., 2004. Revisiting nutrient utilization in the glacial
526 Antarctic: Evidence from a new method for diatom-bound N isotopic analysis.
527 *Paleoceanography* 19, 1–13. doi:10.1029/2003PA000996
528 Robinson, R.S., Kienast, M., Luiza Albuquerque, A., Altabet, M., Contreras, S., De Pol Holz, R.,
529 Dubois, N., Francois, R., Galbraith, E., Hsu, T.C., Ivanochko, T., Jaccard, S., Kao, S.J.,
530 Kiefer, T., Kienast, S., Lehmann, M., Martinez, P., McCarthy, M., Möbius, J., Pedersen, T.,
531 Quan, T.M., Ryabenko, E., Schmittner, A., Schneider, R., Schneider-Mor, A., Shigemitsu,
532 M., Sinclair, D., Somes, C., Studer, A., Thunell, R., Yang, J.Y., 2012. A review of nitrogen
533 isotopic alteration in marine sediments. *Paleoceanography* 27. doi:10.1029/2012PA002321
534 Schubert, C.J., Calvert, S.E., 2001. Nitrogen and carbon isotopic composition of marine and
535 terrestrial organic matter in Arctic Ocean sediments: *Deep Sea Res. Part I Oceanogr. Res.*
536 *Pap.* 48, 789–810. doi:10.1016/S0967-0637(00)00069-8
537 Sciences, C., Brunswick, N., Agency, A., Watershed, S., Hole, W., Seitzinger, S., Harrison, J. a,
538 Böhlke, J.K., Bouwman, a F., Lowrance, R., Peterson, B., Tobias, C., Van Drecht, G.,
539 2006. Denitrification across landscapes and waterscapes: a synthesis. *Ecol. Appl.* 16, 2064–
540 90.
541 Serreze, M.C., Barrett, A.P., Slater, A.G., Woodgate, R.A., Aagaard, K., Lammers, R.B., Steele,
542 M., Moritz, R., Meredith, M., Lee, C.M., 2006. The large-scale freshwater cycle of the
543 Arctic. *J. Geophys. Res. Ocean.* 111. doi:10.1029/2005JC003424
544 Serreze, M.C., Barry, R.G., 2011. Processes and impacts of Arctic amplification: A research
545 synthesis. *Glob. Planet. Change* 77, 85–96. doi:10.1016/j.gloplacha.2011.03.004
546 Solomina, O.N., Bradley, R.S., Hodgson, D.A., Ivy-Ochs, S., Jomelli, V., Mackintosh, A.N.,
547 Nesje, A., Owen, L.A., Wanner, H., Wiles, G.C., Young, N.E., 2015. Holocene glacier
548 fluctuations. *Quat. Sci. Rev.* doi:10.1016/j.quascirev.2014.11.018
549 Stein, R., Boucein, B., Fahl, K., Garcia de Oteyza, T., Knies, J., Niessen, F., 2001.
550 Accumulation of particulate organic carbon at the Eurasian continental margin during late
551 Quaternary times: Controlling mechanisms and paleoenvironmental significance. *Glob.*
552 *Planet. Change* 31, 87–104. doi:10.1016/S0921-8181(01)00114-X
553 Stein, R., Dittmers, K., Fahl, K., Kraus, M., Matthiessen, J., Niessen, F., Pirrung, M., Polyakova,
554 Y., Schoster, F., Steinke, T., Fütterer, D.K., 2004. Arctic (palaeo) river discharge and
555 environmental change: Evidence from the Holocene Kara Sea sedimentary record, in:
556 *Quaternary Science Reviews.* pp. 1485–1511. doi:10.1016/j.quascirev.2003.12.004
557 Stein, R., Fahl, K., 2000. Holocene accumulation of organic carbon at the Laptev Sea continental
558 margin (Arctic Ocean): sources, pathways, and sinks. *Geo-Marine Lett.* 20, 27–36.
559 doi:10.1007/s003670000028
560 Stein, R., Fahl, K., Niessen, F., Siebold, M., 1999. Late Quaternary organic carbon and
561 biomarker records from the Laptev Sea continental margin (Arctic Ocean): implications for
562 organic carbon flux and composition, in: *Land-Ocean Systems in the Siberian Arctic:*

563 Dynamics and History. pp. 635–655.

564 Stein, R., Fahl, K., Schade, I., Manerung, A., Wassmuth, S., Niessen, F., Nam, S. Il, 2017.

565 Holocene variability in sea ice cover, primary production, and Pacific-Water inflow and

566 climate change in the Chukchi and East Siberian Seas (Arctic Ocean). *J. Quat. Sci.* 32, 362–

567 379. doi:10.1002/jqs.2929

568 Stevenson, F.J., Dhariwal, A.P.S., 1959. Distribution of fixed ammonium in soils. *Soil Sci. Soc.*

569 *Am. J.* 23, 121–125.

570 Straub, M., Tremblay, M.M., Sigman, D.M., Studer, A.S., Ren, H., Toggweiler, J.R., Haug,

571 G.H., 2013. Nutrient conditions in the subpolar North Atlantic during the last glacial period

572 reconstructed from foraminifera-bound nitrogen isotopes. *Paleoceanography* 28, 79–90.

573 doi:10.1002/palo.20013

574 Tesdal, J.E., Galbraith, E.D., Kienast, M., 2013. Nitrogen isotopes in bulk marine sediment:

575 Linking seafloor observations with subseafloor records. *Biogeosciences* 10, 101–118.

576 doi:10.5194/bg-10-101-2013

577 Thibodeau, B., Bauch, D., 2016. The impact of climatic and atmospheric teleconnections on the

578 brine inventory over the Laptev Sea shelf between 2007 and 2011. *Geochemistry, Geophys.*

579 *Geosystems* 17, 56–64. doi:10.1002/2015GC006063

580 Thibodeau, B., Bauch, D., Kassens, H., Timokhov, L.A., 2014. Interannual variations in river

581 water content and distribution over the Laptev Sea between 2007 and 2011: The Arctic

582 Dipole connection. *Geophys. Res. Lett.* 41, 7237–7244. doi:10.1002/2014GL061814

583 Thibodeau, B., Bauch, D., Voss, M., 2017a. Nitrogen dynamic in Eurasian coastal Arctic

584 ecosystem: Insight from nitrogen isotope. *Global Biogeochem. Cycles* 31.

585 doi:10.1002/2016GB005593

586 Thibodeau, B., Bauch, H.A., Pedersen, T.F., 2017b. Stratification-induced variations in nutrient

587 utilization in the Polar North Atlantic during past interglacials. *Earth Planet. Sci. Lett.* 457,

588 127–135. doi:10.1016/j.epsl.2016.09.060

589 Werner, K., Müller, J., Husum, K., Spielhagen, R.F., Kandiano, E.S., Polyak, L., 2016. Holocene

590 sea subsurface and surface water masses in the Fram Strait: Comparisons of temperature

591 and sea-ice reconstructions. *Quat. Sci. Rev.* 147, 194–209.

592 doi:10.1016/j.quascirev.2015.09.007

593 Werner, K., Spielhagen, R.F., Bauch, D., Hass, H.C., Kandiano, E., 2013. Atlantic Water

594 advection versus sea-ice advances in the eastern Fram Strait during the last 9 ka: Multiproxy

595 evidence for a two-phase Holocene. *Paleoceanography* 28, 283–295.

596 doi:10.1002/palo.20028

597 Xiao, X., Stein, R., Fahl, K., 2015. MIS 3 to MIS 1 temporal and LGM spatial variability in

598 Arctic Ocean sea ice cover: Reconstruction from biomarkers. *Paleoceanography* 30, 969–

599 983. doi:10.1002/2015PA002814

600 Zakharov, V.F., 1966. The role of flaw leads off the edge of fast ice in the hydrological and ice

601 regime of the Laptev Sea. *Oceanology* 6, 815–821.

602

603